

Gamma Rays from the Proton Bombardment of Mg^{24}

A. E. LITHERLAND, E. B. PAUL, G. A. BARTHOLOMEW, AND H. E. GOVE
Chalk River Laboratory, Atomic Energy of Canada Limited, Chalk River, Ontario, Canada

(Received December 27, 1955)

The reactions $Mg^{24}(p,\gamma)Al^{25}$, $Q=2.29$ Mev, and $Mg^{24}(p,p'\gamma)Mg^{24}$, $Q=-1.37$ Mev, have been measured for proton energies in the range 0.40 to 3.0 Mev. New levels in Al^{25} have been found at 1.61, 3.44, 4.90, 5.06, 5.10 Mev, and possibly at 5.09 Mev. Appropriate angular distribution measurements of proton-capture gamma rays and gamma rays from inelastic proton scattering, combined with previous measurements by other investigators, allow unambiguous spin and parity assignments to be made for all known levels in Al^{25} up to 4.7 Mev with the exception of those at 1.61, 2.51, and 3.44 Mev, where the assignments are less certain. The gamma-ray branching ratios for all the levels up to 4.7 Mev have been measured, as well as absolute values of the product of Γ_p/Γ and the partial widths for primary gamma transitions and inelastic proton scattering for states above the proton binding energy. In several cases, intensity ratios of $E2-M1$ mixtures were obtained. An interpretation of some of the results based on a collective model of the Al^{25} nucleus is given.

INTRODUCTION

THE states of Al^{25} reached by proton bombardment of Mg^{24} have been studied by the elastic scattering of protons by Mooring *et al.*¹ Spin, parity, and reduced width assignments have been made² by analyzing the shape of the yield curve. The $Mg^{24}(d,n)Al^{25}$ stripping reaction has been studied by Goldberg,³ who, on the basis of the theory of the angular distribution of the stripping reaction products, has made spin and parity assignments to several of the lower levels. The $Mg^{24}(p,\gamma)Al^{25}$ reaction has been observed at the 225-kev and 418-kev resonances by several groups of workers listed by Endt and Kluyver,⁴ and at the 825-kev resonance by Green *et al.*⁵ and Green *et al.*⁶ The latter have also studied the gamma-ray spectrum at this resonance. The gamma-ray spectrum has been studied by Casson⁷ and by Craig⁸ at the 222-kev resonance.

The mirror nucleus, Mg^{25} , has been studied by several groups,⁴ and the positions and properties of the levels compared with those of Al^{25} .

In this paper, the properties of the states of Al^{25} have been further investigated by extending the studies of the proton capture gamma rays and gamma rays from inelastic scattering to a bombarding energy of 3 Mev. All resonances observed by Mooring *et al.*¹ up to this proton energy have been observed to decay by gamma-ray emission to various lower states of Al^{25} , and in the case of the resonances at 2.01 Mev and 2.40 Mev, a 1.37-Mev gamma ray arising from the reaction $Mg^{24}(p,p'\gamma)$, $Q=-1.37$ Mev, has also been observed. New resonances have been found for proton capture gamma rays at 1.20 Mev and for 1.37-Mev gamma rays from inelastic scattering at 2.72, 2.89, and 2.93 Mev,

and possibly at 2.92 Mev. Those at 2.89 and 2.93 Mev have also been observed at Duke University.⁹ The gamma-ray emission partial widths of the primary gamma rays have been measured at each of the resonances, and the branching ratios of the subsequent cascading radiations have been measured. Angular distribution measurements on the capture gamma rays and the gamma rays from inelastic proton scattering have been made, and spins and parities have been determined for all the states observed in Al^{25} . These spin and parity assignments are unambiguous for levels below 4.7 Mev except for the levels at 1.61, 2.51, and 3.44 Mev.

APPARATUS

The Chalk River electrostatic generator provided a beam of protons in the energy range 400 kev to 3.0 Mev. The machine voltage in this range of energies was stabilized to approximately ± 1 kilovolt by means of a variable corona load. The proton beam passed through a one-eighth inch diameter hole in a sheet of tantalum 45 inches from the target, producing a beam spot about one-quarter inch in diameter on the target. Above 800 kev, the H^+ beam was used, while below this the H_2^+ and H_3^+ beams were employed. The proton current incident on the target backing was measured by a current integrator similar to that described by Gittings.¹⁰

The protons bombarded a thin (~ 10 kev at $E_p=1.5$ Mev) enriched target of isotopic constitution 99.3% Mg^{24} deposited on a 0.02-inch thick tantalum backing. The enriched Mg^{24} isotope evaporated on the backing was obtained from the Atomic Energy Research Establishment, Harwell.

The gamma rays were measured in two sodium iodide scintillation counters, each consisting of a NaI(Tl) crystal five inches in diameter and four inches long, coupled to a Dumont K-1198 photomultiplier. The large NaI(Tl) crystals were mounted in a manner

¹ Mooring, Koester, Goldberg, Saxon, and Kaufmann, *Phys. Rev.* **84**, 703 (1951).

² L. J. Koester, *Phys. Rev.* **85**, 643 (1952).

³ E. Goldberg, *Phys. Rev.* **89**, 760 (1953).

⁴ P. M. Endt and J. C. Kluyver, *Revs. Modern Phys.* **26**, 95 (1954).

⁵ Green, Harris, and Cooper, *Phys. Rev.* **96**, 817(A) (1954).

⁶ Green, Singh, and Willmott, *Phil. Mag.* **46**, 982 (1955).

⁷ H. Casson, *Phys. Rev.* **89**, 809 (1953).

⁸ D. S. Craig, *Phys. Rev.* **101**, 1479 (1956).

⁹ H. W. Lewis (private communication).

¹⁰ H. T. Gittings, *Rev. Sci. Instr.* **20**, 325 (1949).

similar to that used by Foote and Koch.¹¹ The output pulses were first delay-line shaped by a preamplifier mounted in the same box as the crystal and multiplier assembly, and, after passing through 50 feet of cable, were amplified by a linear amplifier. The pulses were fed from the amplifier either directly to a 30-channel pulse-height analyzer, or to the 30-channel analyzer after first passing through a linear gate circuit. This gate circuit was opened by pulses selected, by means of a single-channel analyzer, from a narrow band in the pulse height spectrum from the other crystal. By means of the latter arrangement, it was possible to study the gamma rays in one crystal in coincidence with a particular gamma ray in the other crystal. The coincidence resolving time used in the experiments to be described was about two microseconds.

The target chamber and angular distribution assembly was essentially the same as that used by Bartholomew *et al.*,¹² with the addition of shielding around each of the sodium iodide crystals, and is shown schematically in Fig. 1. The shielding, which consisted of a layer of lead about two inches thick and weighing about 800 lb, was found necessary to reduce the radioactive background from the surroundings. In particular, the 1.48-Mev gamma ray from the disintegration of K^{40} was reduced by the lead shielding. Even with the lead shielding, a background was observed which interfered with the study of the weaker gamma rays from the reactions. The crystal assemblies were mounted on the angular distribution apparatus in a manner which enabled them to be set at angles between $\cos\theta=1.0$ and -0.8 with respect to the proton beam. One crystal was used either as a monitor in angular distribution experiments or, in coincidence experiments, with the other crystal. Both crystals with associated lead shielding and preamplifiers were supported in a manner which enabled the distance between the crystal and the target to be varied.

EXPERIMENTAL PROCEDURE AND METHOD OF ANALYSIS

In general, no collimation was used to define the gamma-ray beam from the target to the sodium iodide crystals because of the low yield of the gamma radiations studied. The line shape for monoenergetic gamma rays emitted from a point source 6.2 inches from the front face of the crystal was measured as a function of gamma-ray energy with the following sources: $N^{15}(p,\alpha\gamma)$ (4.44 Mev), $Be^9(p,\alpha\gamma)$ (3.57 Mev), Na^{24} (2.76 Mev), ThC'' (2.61 Mev), Pr^{144} (2.19 Mev), Na^{22} (1.28 Mev), Zn^{65} (1.12 Mev), Mn^{56} (0.822 Mev), Na^{22} (0.511 Mev). The spectra for four of these are shown in Fig. 2(a). It is to be noted that, while the total absorption peak predominates at most energies, the single annihilation quantum escape peak becomes comparable at the higher

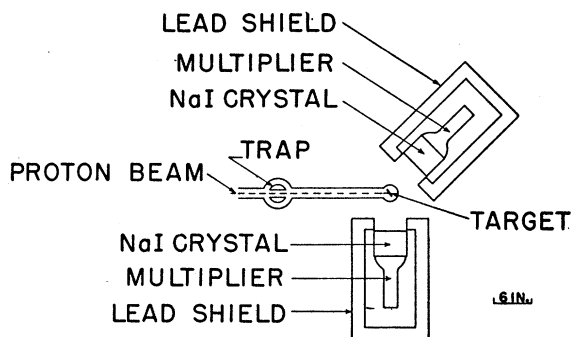


FIG. 1. Schematic view of the apparatus.

energies. The escape peak could be reduced if good collimation were possible.

The absolute efficiency, defined for convenience as the counts contained in the total absorption peak per photon emitted from a point source 6.2 inches from the front face of the crystal, was determined at three energies by using a calibrated Na^{22} source and by measuring the thick-target yield¹³ of 6.13-Mev gamma rays from the $F^{19}(p,\alpha\gamma)O^{16}$ reaction at $E_p=1.0$ Mev. The shape of the yield curve between these points was obtained by using a Sc^{46} and Na^{24} source. This absolute efficiency curve is shown in Fig. 2(b).

The yield curve for the $Mg^{24}(p,\gamma)Al^{25}$ reaction was measured for a range of proton energies between 0.8 and 2.0 Mev by counting, for a given number of microcoulombs of H^+ beam striking the target, the number of pulses corresponding to gamma rays in the energy ranges either from 1.5 to 2.3 Mev or from 2.3 to 3.0 Mev entering one of the counters fixed at 90° to the beam. For proton energies from 2.0 to 3.0 Mev, the yield of 1.37-Mev gamma rays from the $Mg^{24}(p,p'\gamma)Mg^{24}$ reaction was measured. Some measurements in the region of the 0.825-Mev resonance were made using the H_2^+ ion beam, but it was found that the natural deuterium component was quite troublesome. In the range of proton energies from 0.40 to 0.85 Mev, the yield of gamma rays between 0.7 and 1.1 Mev was measured employing the H_3^+ beam. The yield curves are shown in Figs. 3 and 4.

At each resonance, the gamma-ray spectrum was measured with the front face of the crystal at the standard 6.2 inches from the target center. This spectrum was subsequently corrected by subtracting background spectra determined by separate measurements. This background was partly due to natural radioactivity which could be measured by turning the generator off. In addition, other sources of background in the energy range 0.51 to 4.0 Mev were encountered. Background gamma rays produced by the proton beam striking the magnet box, energy defining slits, and aperture were considerably reduced by a lead shielding wall between

¹¹ R. S. Foote and H. W. Koch, *Rev. Sci. Instr.* **25**, 746 (1954).

¹² Bartholomew, Brown, Gove, Litherland, and Paul, *Can. J. Phys.* **33**, 441 (1955).

¹³ F. Ajzenberg and T. Lauritsen, *Revs. Modern Phys.* **27**, 77 (1955).

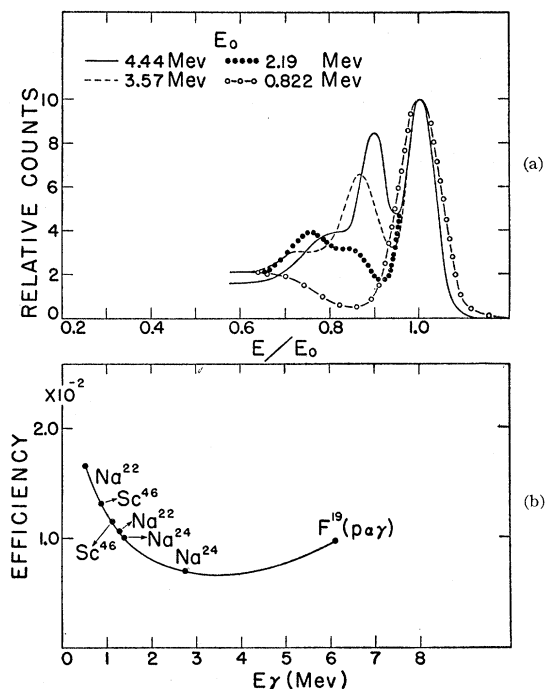


FIG. 2. The upper curves show the shapes of pulse-height distributions for monochromatic gamma rays of four different energies emitted from point sources 6.2 in. from the front face of the 5 in. diameter by 4 in. long sodium iodide scintillation spectrometer with no collimation. The lower curve shows the absolute efficiency of the spectrometer as a function of gamma-ray energy for the total absorption peak in the gamma-ray spectrum employing the above geometry.

the experimental area and the sources of radiation. Contaminant gamma rays from the target that were observed were those from the reactions $\text{Na}^{23}(p,\alpha\gamma)\text{Ne}^{20}$, $\text{N}^{15}(p,\alpha\gamma)\text{C}^{12}$, $\text{F}^{19}(p,\alpha\gamma)\text{O}^{16}$, and also from proton capture by C^{12} at the 0.46- and 1.7-Mev resonances. The background from these carbon gamma rays increased with time due to a slow buildup of carbon on the target, which was not completely eliminated by a liquid nitrogen trap situated near the target. These sources of background could be estimated by measuring the spectrum just above and below a resonance.

The spectra so obtained varied considerably from resonance to resonance. By using the known shapes of the gamma-ray lines, it was possible to analyze the spectrum into its component gamma rays and, with the aid of the efficiency curve of Fig. 2(b), to determine the relative intensities of the gamma rays at a given angle. The absolute intensity for a particular gamma ray was determined from a knowledge of the total number of protons striking the target, the target thickness, the absolute efficiency of the counter for the gamma ray, and its angular distribution. The total number of protons was measured by the beam integrator. A suppressor grid at a potential of -300 volts with respect to the target was located in front of, and close to, the target to minimize the effect of electrons

either emitted from the target or traveling along with the beam. At all the resonances except the ones at $E_p = 1.62$ Mev and 2.93 Mev, the target thickness was much greater than the known² natural widths of the resonances; and hence the thick target yield was obtained, and from this the quantity $(J + \frac{1}{2})\Gamma_p\Gamma_\gamma/\Gamma$, where J is the spin of the resonance and Γ_p , Γ_γ , and Γ the partial width for formation by protons, decay by a particular gamma ray, and the total width respectively.¹⁴ In this calculation, the stopping cross section for air was obtained from the compilation of Bethe,¹⁵ and the relative stopping power of Mg was assumed to be 1.5.¹⁵ The target thickness at the broad 1.62-Mev resonance was estimated from the observed width of the narrow resonance at 1.66 Mev to be 9.5 kev.

Angular distributions of the principal gamma rays were measured at all the resonances observed. This was accomplished by recording the appropriate portions of the spectrum, at various angles with respect to the proton beam, in one of the crystals. The second crystal, fixed at 270° to the beam, was used as a monitor. The front faces of the counters for these measurements were 6 to 10 inches from the target center. An estimate of the geometrical correction to be applied to the experimental angular distributions was obtained by measuring the angular distribution of the 1.37-Mev gamma ray from the reaction $\text{Mg}^{24}(p,p'\gamma)\text{Mg}^{24}$ for a series of distances between the crystal front face and the target center varying from 4.6 to 10.1 inches. The resonance chosen for this test was that at $E_p = 2.40$ Mev, where the distribution of this gamma ray has large P_2 and P_4 coefficients in the Legendre polynomial fit to the data. These Legendre polynomial fits up to P_4 were made on the Ferranti computer at the University

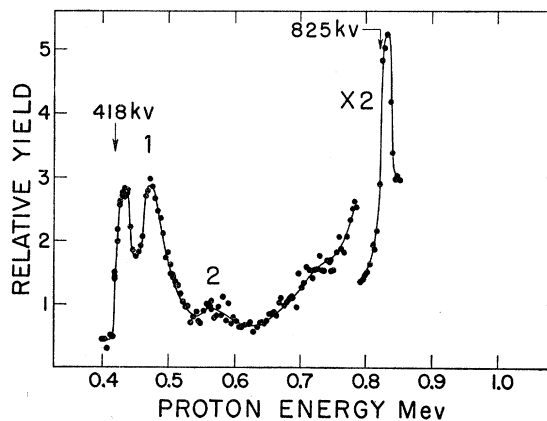


FIG. 3. The yield of gamma rays of energies between 0.7 and 1.1 Mev from $\text{Mg}^{24}(p,\gamma)\text{Al}^{25}$, using the H_3^+ beam for proton energies between 0.40 and 0.85 Mev. Resonances 1 and 2 are from contaminants on the target.

¹⁴ Fowler, Lauritsen, and Lauritsen, *Revs. Modern Phys.* **20**, 236 (1948).

¹⁵ H. A. Bethe, Brookhaven National Laboratory Report BNL-T-7, June, 1949 (unpublished); M. S. Livingston and H. A. Bethe, *Revs. Modern Phys.* **9**, 245 (1937).

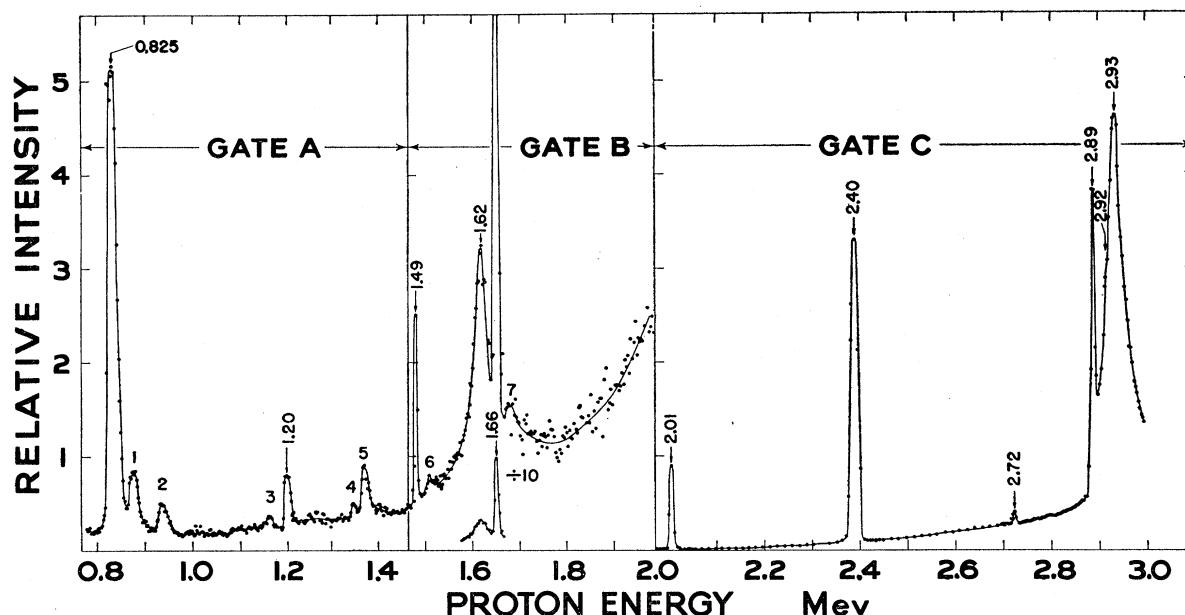


FIG. 4. The yield of gamma rays from the reactions $Mg^{24}(p,\gamma)Al^{25}$ and $Mg^{24}(p,p'\gamma)Mg^{24}$ for the proton energy range 0.80 to 3.05 Mev. For proton energies between 0.80 and 1.46 Mev, gamma rays of energies between 1.5 and 2.3 Mev were recorded (Gate A). For proton energies between 1.46 and 2.0 Mev, gamma rays of energies between 2.3 and 3.0 Mev were recorded (Gate B). For proton energies above 2.0 Mev, the yield of 1.37-Mev gamma rays from the $Mg^{24}(p,p'\gamma)Mg^{24}$ reaction was recorded (Gate C). The numbered resonances 1 to 7 are from contaminants on the target.

of Toronto. The results of this measurement indicated that the P_2 coefficient was attenuated by 10% and the P_4 by 20% at the closest distance employed. Only the angular distributions of the 1.37-Mev gamma ray from inelastic proton scattering were fitted with Legendre polynomials by least squares on the Ferranti computer. The remaining distributions, plotted semilogarithmically, were compared to standard curves similarly plotted, and the best fit and limiting values were estimated. The differences between the best fit and the limiting values, in these cases, will be referred to as standard deviations even though they are not mathematically well defined.

At some resonances, coincidence measurements were made to determine the decay scheme. For these measurements, the crystals were generally placed at 90° and 270° to the beam, respectively, and as close to the target as possible. A narrow band containing the full-energy peak of a gamma ray in the spectrum recorded by one counter was selected by a single-channel analyzer. The pulses in this channel opened a gate circuit which permitted coincident pulses from the other crystal to be recorded on the 30-channel analyzer. This geometry was not satisfactory if one or both of the gamma rays in coincidence had an energy near 0.5 Mev. Since the first two states of Al^{25} decay partly by the emission of gamma rays near this energy, this situation occurred in this experiment. In this case, if, for example, the single channel is set on a 0.5-Mev gamma ray and the counters are 180° apart, the coincidence spectrum will show a 0.5-Mev gamma-ray peak from pair production by the

emitted gamma rays in the target backing and chamber, as well as from the positron decay of Al^{25} . The single-annihilation-escape peak of each gamma ray of sufficient energy will also appear in coincidence with a gamma ray of energy 0.5 Mev. Hence experiments involving coincidences with a 0.5-Mev gamma ray were performed by placing the two crystals with their axes 90° apart and with lead arranged to shield them from each other. In some cases, triple correlation measurements were made to give additional information about spins and parities of bound levels. This involved measuring coincidences between pairs of gamma rays with one counter fixed at 270° and the other rotated between 0° and 90° . For these measurements the counters were moved back to a distance of about seven inches between the crystal front face and the target.

Theoretical expressions for the four types of angular distribution that have been measured are obtained from Sharp *et al.*¹⁶ and from tables prepared by Ferguson, Rutledge, and Litherland.¹⁷ These four distributions are as follows: in proton capture gamma-ray processes, the correlation between the primary gamma ray and the proton, the correlation between a second gamma ray and the proton with the primary unobserved, and triple correlations, that is, coincidence correlations between the primary and secondary gamma ray with

¹⁶ Sharp, Kennedy, Sears, and Hoyle, Atomic Energy of Canada Limited, Chalk River Project, A.E.C.L. No. 97, December, 1953 (unpublished).

¹⁷ A. J. Ferguson and A. E. Litherland, Phys. Rev. **99**, 1654(A) (1955); A. J. Ferguson and A. R. Rutledge, Atomic Energy of Canada Limited, Chalk River Project, CRP-615 (unpublished).

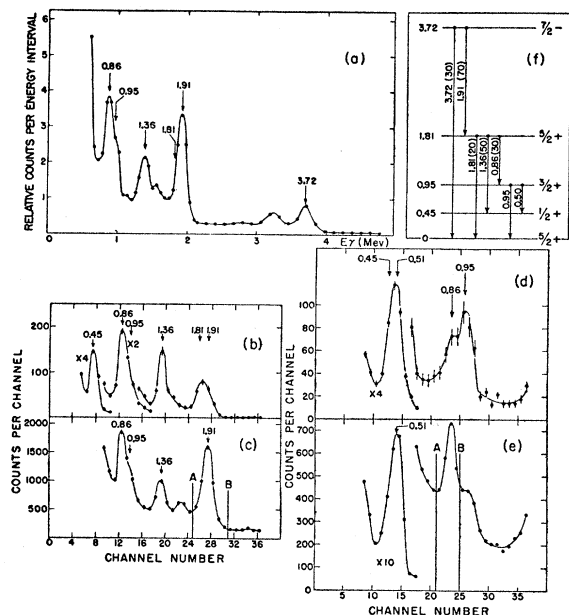


FIG. 5. Measurements of spectra at the 1.49-Mev resonance. (a) A portion of the direct spectrum of gamma rays. The energies of the principal gamma rays are shown. (b) A portion of the spectrum of gamma rays in coincidence principally with gamma rays of about 1.9 Mev. (c) Part of the direct spectrum showing the limits *A* and *B* of the single-channel analyzer which gated the coincidence spectrum (b). (d) A portion of the spectrum of gamma rays in coincidence principally with gamma rays of about 0.86 Mev. (e) Part of the direct spectrum showing the limits *A* and *B* of the single-channel analyzer which gated the coincidence spectrum (d). (f) The decay scheme for the 3.72-Mev state in Al^{25} . The gamma-ray energies are listed together with branching ratios in brackets.

respect to the proton beam; and for inelastic proton scattering followed by gamma radiation, the correlation between the gamma ray and the proton beam with the inelastic protons unobserved. The theoretical analysis is simplified because the target nucleus has zero spin, and hence no channel spin or orbital mixtures are involved for the incident protons.

EXPERIMENTAL RESULTS

In this section the experimental data for each resonance will be presented, and conclusions regarding spins, parities, branching ratios, partial widths, and multipole mixtures will be given. Some of the measurements to be described have been reported previously.¹⁸

In the yield curve of Fig. 3, resonances corresponding to excited states in Al^{25} occur at proton energies of 0.418 and 0.825 Mev, and in Fig. 4, at 0.825, 1.20, 1.49, 1.62, 1.66, 2.01, 2.40, 2.72, 2.89, and 2.93 Mev. A possible resonance also occurs at 2.92 Mev. Resonances numbered 1 and 2 in Fig. 3 are from the reactions $\text{C}^{12}(p,\gamma)\text{N}^{13}$ at 457 kev and $\text{C}^{13}(p,\gamma)\text{N}^{14}$ at 550 kev,

¹⁸ Litherland, Paul, Bartholomew, and Gove, *Phys. Rev.* **99**, 644(A) (1955); Paul, Bartholomew, Gove, and Litherland, *Phys. Rev.* **99**, 644(A) (1955); Bartholomew, Gove, Litherland, and Paul, *Phys. Rev.* **99**, 1649(A) (1955).

respectively. The numbered resonances in Fig. 4 are also contaminants, 1, 2, 5, and 7 from the reaction $\text{F}^{19}(p,\alpha\gamma)\text{O}^{16}$ at $E_p=0.874, 0.935, 1.355,$ and 1.670 Mev, respectively, and 3 from the reaction $\text{Na}^{23}(p,\alpha\gamma)$ at $E_p=1.166$ Mev. The resonances 4 and 6 are of unknown origin. They are so weak as to make a detailed investigation difficult. The resonance at 2.92 Mev which appears as an inflection on the side of the 2.93-Mev resonance is not certain although it does correspond in energy to a discontinuity in the elastic yield curve of Mooring *et al.*¹ The possible level in Al^{25} at an excitation energy of 2.92 Mev observed by Goldberg,³ which would correspond to a proton energy of about 660 kev, was not observed in the yield curve of Fig. 3. All the $\text{Mg}^{24}+p$ resonances shown in Fig. 4 except those at 1.20, 2.72, 2.89, and 2.93 Mev were observed by Mooring *et al.*,¹ and their total widths have been reported by Koester.² At the 0.418-, 1.20-, 2.72-, and 2.89-Mev resonances the total widths appear to be less than the target thickness (10 kev at 1.5 Mev). The 2.93-Mev resonance has a total width of about 50 kev.

The resonance at $E_p=1.49$ Mev illustrates some special points, and it will be discussed first. Subsequent resonances will be described in order of increasing proton energy.

1.49-Mev Resonance

Part of the direct spectrum of gamma rays following proton capture in Mg^{24} at this resonance measured at 90° to the beam is shown in Fig. 5(a). The following gamma rays are observed: 3.72 Mev, a 1.91- and 1.81-Mev complex unresolved, 1.36 Mev, a 0.95- and 0.86-Mev complex partially resolved, and a 0.5-Mev complex unresolved, not shown in Fig. 5(a). That the peak around 1.9 Mev actually consists of two gamma rays was clear from an examination of the widths at half-maximum as a function of angle with respect to the proton beam. This varied from about 8.5% to 12.5% while, for a single gamma ray of this energy, it would be 8%. The quoted energies for the two components are not obtained from these data, but have been assumed from the energy levels of Al^{25} quoted by Endt and Kluyver.⁴

Coincidence spectra were measured in three different ways. First, with the two counters set at 90° and 270° , respectively to the beam, the single-channel pulse-height analyzer was set to include the 1.91, 1.81-Mev complex measured by one crystal, and the spectrum of gamma rays in coincidence with these was recorded from the other. This is illustrated in Figs. 5(b) and 5(c). The coincidence spectrum showed all the gamma rays found in the corresponding part of the direct spectrum, although in different proportions. Secondly, a coincidence spectrum was measured in the same geometry with one counter gated principally to register gamma rays in coincidence with the 0.86-Mev gamma ray which is only partially resolved from the 0.95-Mev. This is shown in Figs. 5(d) and 5(e). The 0.86-Mev gamma ray

is considerably reduced in intensity over the 0.95 Mev in the coincidence spectrum, compared to the situation observed in the direct spectrum. Finally, the counters were set at 0° and 90°, respectively, to the beam, and shielded from each other. One counter was gated to register gamma rays in coincidence with the 0.5-Mev complex. This indicated that a gamma ray of about 0.5 Mev was in coincidence with another of about the same energy.

From these measurements the decay scheme can be constructed as shown in Fig. 5(f). The 3.72- and 1.91-Mev gamma rays are primary radiations feeding the ground state and 1.81-Mev state in Al²⁵, respectively. This latter state decays by a direct transition to ground, to the first excited state of 0.45 Mev by a gamma ray of energy 1.36 Mev, and to the second excited state at 0.95 Mev by a 0.86-Mev gamma ray. The 0.95-Mev state decays by a direct transition to ground and by a 0.5-, 0.45-Mev cascade through the first excited state. A better measurement of the branching ratio of the 0.95-Mev state was made at the 1.62-Mev resonance. This decay scheme accounts for all the gamma rays observed in the direct and coincidence spectra, and is consistent with the known⁴ low-lying levels in Al²⁵. It should be remarked that, in general, no attempt was made to measure gamma-ray energies to an accuracy of better than ±20 kev, and in most cases energies quoted correspond to the excitation energies quoted in Endt and Kluver.⁴

In order to determine spins and parities of some of the levels in Al²⁵ observed at this resonance, a number of angular distribution measurements of gamma rays with respect to the proton beam was made. These are summarized in Table I, which lists for each the coefficient of P₂ and P₄ in the Legendre polynomial expansion of the distribution, and are as follows: (1) the direct correlation of the ground state transition (3.72 Mev), which is shown in Fig. 6(a); (2) the direct correlation of the transition to the 1.81-Mev state (1.91 Mev) shown in Fig. 6(b); (3) the direct correlation of the transition between the 1.81-Mev and the 0.45-Mev

TABLE I. Angular distribution measurements at the 1.49-Mev resonance. The first four distributions are direct correlations with respect to the proton beam of the gamma ray whose energy is given in Column 3 in Mev. The last three are triple correlations with the gamma rays in Column 2 measured in a counter fixed at 270° to the beam, and those in Column 3, in coincidence with the former, measured in the moving counter for angles between 0° and 180°. The last two columns list the coefficients of P₂ and P₄ and their standard deviations (S.D.) in the Legendre polynomial expansions of the distributions.

Dist. No.	Energy of gamma ray measured in counter		a ₂ /a ₀		a ₄ /a ₀	
	Fixed at 270°	Moving		S.D.		S.D.
1		3.72	-0.40	0.05		
2		1.91	-0.40	0.10		
3		1.36	+0.47	0.10	-0.32	0.10
4		1.81	+0.60	0.30		
5	1.81+1.91	1.81+1.91	+0.40	0.30		
6	1.91	1.36	+0.60	0.20	-0.40	0.20
7	1.91	0.86	+0.05	0.15		

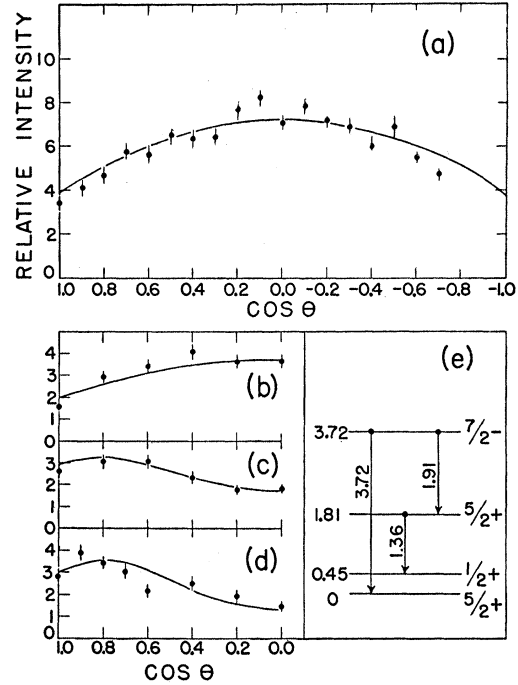


FIG. 6. Measurements of angular distributions at the 1.49-Mev resonance. (a) The direct correlation of the 3.72-Mev gamma ray with respect to the proton beam. The solid line represents $P_0 - 0.40P_2$. (b) The direct correlation of the 1.91-Mev gamma ray with respect to the proton beam. The solid line represents $P_0 - 0.40P_2$. (c) The direct correlation of the 1.36-Mev gamma ray with respect to the proton beam with the intermediate 1.91-Mev gamma ray unobserved. The solid line represents $P_0 + 0.47P_2 - 0.32P_4$. (d) The triple correlation of coincidences between the 1.91-Mev gamma ray measured in a counter fixed at 270° to the beam and the 1.36-Mev gamma ray measured in a counter moved between $\theta = 0^\circ$ and 90° to the beam. The solid line represents $P_0 + 0.6P_2 - 0.4P_4$. (e) An energy level diagram showing the gamma rays studied.

state (1.36 Mev) with the intermediate radiation (1.91 Mev) unobserved, shown in Fig. 6(c); (4) the direct correlation of the transition between the 1.81-Mev state and ground with the intermediate radiation unobserved; and finally three triple correlations (5, 6, and 7) which were measured simultaneously. In this measurement one counter was fixed at 270° to the beam with its single-channel analyzer set on the 1.91+1.81-Mev gamma rays. The coincidence spectrum comprising gamma rays of 1.91 and 1.81 Mev unresolved, 1.36 Mev, and 0.95 and 0.86 Mev partially resolved, was recorded as a function of angle between 0° and 90° by the movable counter. The results for the 1.36-Mev gamma ray are shown in Fig. 6(d). The 0.86-Mev gamma ray was resolved graphically from the 0.95-Mev to obtain the P₂ coefficient listed in Table I which, as a consequence, is quite inaccurate.

From these results some conclusions about the spin and parity of the 3.72- and 1.81-Mev levels in Al²⁵ can be drawn. The spins and parities of the ground and first excited states of Al²⁵ have been shown³ to be (5/2, 3/2)+ and 1/2+, respectively. Measurements

TABLE II. Spin and parity combinations for the 3.72- and 1.81-Mev levels which can be excluded from the angular distribution measurements. The tabulated numbers refer to the corresponding distributions in Table I. The row headings refer to possible spins and parities for the 3.72-Mev state, and the column headings to those for the 1.81-Mev state. The presence of a tabulated number indicates that the comparison of that distribution with theory excludes the corresponding spin combination. The asterisks indicate that the combination is permitted.

J_π for 3.72-Mev level	J_π for 1.81-Mev level		
	5/2+	3/2+	3/2-
9/2+	1, 2	1, 3, 6	1, 3, 6
7/2+	*	2, 3, 6	3, 6
7/2-	*	3, 6	2, 3, 6
5/2+	3	3, 6	3, 6
5/2-	1, 2, 3	1, 3, 6	1, 3, 6
3/2+	3	3, 6	3, 6
3/2-	1, 2, 3	1, 2, 3, 6	1, 3, 6

discussed below at the 0.825-Mev resonance establish the ground state spin to be 5/2+. The level at 1.81-Mev decays to the first excited state (by a gamma ray of 1.36 Mev). Hence the spin and parity of the 1.81-Mev state is 5/2+, 3/2±, or 1/2±. The assignment of 5/2- and higher is excluded because this would require the radiation to be $M2$ or higher, and it is unlikely that these would compete to any appreciable extent with $E1$, $M1$, or $E2$ transitions. The assignments 1/2± are excluded because distributions 3 and 4 (Table I) show that the radiations from the 1.81-Mev state are not spherically symmetric. Similarly, since the level at 3.72-Mev decays to the ground state (5/2+) of Al^{25} , it can have spin and parity 9/2+, 7/2±, 5/2±, or 3/2±. Again 1/2± is excluded because distributions 1 and 2 (Table I) are not spherically symmetric. Table II lists possible spin-parity combinations between the 3.72-Mev and 1.81-Mev states. The numbers in each square, which refer to the angular distributions of Table I, show that the corresponding combination is not allowed by the measurement. The observation of a P_4 term in distribution 3 requires that the spin of both states be equal to or greater than 5/2, while the P_4 term observed in distribution 6 requires that this condition apply only to the 1.81-Mev state. In addition, the combination 5/2± for the 3.72-Mev state and 5/2 for the 1.81-Mev state is eliminated by distribution 3, since the theory for this predicts a positive P_4 coefficient. The direct correlations 1 and 2 are readily compared to theory, and eliminate all the combinations shown. The only assumption on which the conclusions of Table II are based is that only $E1$, $M1$, and $E2$ radiations participate. This in itself eliminates four of the combinations in Table II. From this analysis the spin and parity assignments for the 3.72- and 1.81-Mev states in Al^{25} are 7/2± and 5/2+, respectively. Distributions 4, 5, and 7 are consistent with these assignments.

The analysis² of the elastic scattering of protons¹ by Mg^{24} at this resonance indicates that it is formed by f -waves, and hence is 5/2- or 7/2-. There may be a little uncertainty in this assignment because the target

thickness was greater than the natural width of the resonance. However, combined with the present results, an assignment of 7/2- to the 3.72-Mev state is strongly favored.

Using these assignments, it now becomes possible to compute the ratio of intensities of $E2$ to $M1$ in both the 1.81- and 0.86-Mev gamma rays by comparing the appropriate experimental P_2 coefficients to the theoretical.¹⁶ In the case of the 1.81-Mev radiation, distribution 4 gives an $E2$ to $M1$ intensity ratio, x^2 , in the range 0.002 to 1.0 with a phase difference of 180°,¹⁹ and distribution 5 is consistent with this. For the 0.86-Mev radiation, distribution 7 gives a ratio from 0.02 to 0.07, and again a phase difference of 180°. The other range of values for x^2 is eliminated because it would require a large positive P_4 term for distribution 7, which was not observed.

In order to obtain branching ratios, the relative

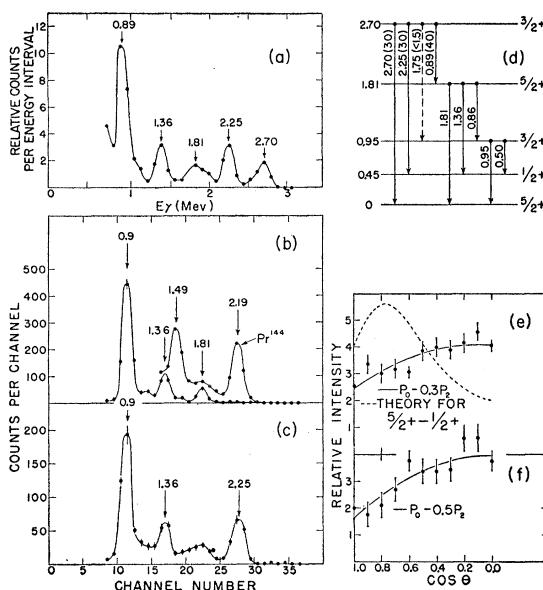


FIG. 7. Measurements at the 418-kev resonance. (a) A portion of the direct spectrum of gamma rays. The energies of the principal gamma rays are shown. (b) A portion of the spectrum of gamma rays in coincidence principally with the peak in the direct spectrum of 0.89 Mev. The direct spectrum from Pr^{144} is shown for comparison. (c) A portion of the spectrum of gamma rays in coincidence principally with gamma rays of about 0.5 Mev. (d) The decay scheme for the 2.70-Mev state in Al^{25} . The gamma-ray energies are listed together with branching ratios in brackets. (e) The direct correlation of the 2.25-Mev gamma rays with respect to the proton beam. The dotted line is the theoretical distribution $P_0 + (4/7)P_2 - (4/7)P_4$ which would arise from a 5/2+ → 1/2+ gamma transition. (f) The direct correlation of the 2.70-Mev gamma rays with respect to the proton beam.

¹⁹ In angular correlations between the primary gamma rays and the proton beam, the phase differences quoted in this paper for $M1-E2$ multipole mixtures, which are based on reference 16, should be subtracted from 180° to make them agree with those of L. C. Biedenharn and M. E. Rose [Revs. Modern Phys. 25, 729 (1953)]. Statements in reference 16 that its definitions of $M1-E2$ phase differences agree with those of Biedenharn and Rose are incorrect [see R. Huby, Proc. Phys. Soc. (London) A67, 1103 (1954)]. A corresponding correction can be made for the other types of correlation measured.

TABLE III. The tabulated numbers are values of $\gamma = \Gamma_p \Gamma_\gamma / \Gamma$ for the reaction $Mg^{24}(p, \gamma)Al^{25}$ in ev except for the last column, which lists $(J + \frac{1}{2}) \Gamma_p \Gamma_{p'}/\Gamma$ in ev for the reaction $Mg^{24}(p, p' \gamma)Mg^{24}$, $Q = -1.37$ Mev. Row headings give the excitation energy in Mev and the spin and parity of the initial state in Al^{25} , and the column headings list the same quantities for the final state.

Initial \ Final	0 5/2+	0.45 1/2+	0.95 3/2+	1.61 7/2+	1.81 5/2+	2.51 1/2+	2.70 3/2+	$(J + \frac{1}{2})$ $\times (\Gamma_p \Gamma_{p'}/\Gamma)$
2.51 1/2+	$\leq 0.0002^a$	0.012 ^a	0.0017 ^a					
2.70 3/2+	0.004	0.004	≤ 0.0002		0.006			
3.09 3/2-	0.014	0.084	0.010		≤ 0.002			
3.44 9/2+	0.0005			0.005				
3.72 7/2-	0.004	≤ 0.0005	≤ 0.0005	≤ 0.0001	0.008			
3.85 1/2-		0.15	0.30			0.07		
3.88 5/2+	0.005	0.003	0.037				0.01	
4.22 3/2+	≤ 0.01	0.18	0.16					60
4.60 5/2+	≤ 0.001	≤ 0.02	0.06					350
4.90 $\geq 5/2$								12
5.06 $\geq 5/2$								184
5.10 $\geq 5/2$								3330

^a D. S. Craig (to be published).

intensities of the full energy peaks of the various gamma rays observed in the spectra of Figs. 5(a) and 5(b) were measured. Using the efficiency curve of Fig. 2(b) and the measured angular distributions of Table I, the branching ratios were calculated and are shown in Fig. 5(f) in brackets following the gamma-ray energy.

The values of $\gamma = \Gamma_p \Gamma_\gamma / \Gamma$ for the two primary radiations of 3.72 Mev and 1.91 Mev have been measured to be 0.0036 and 0.0084 ev, respectively, with estimated accuracies of $\pm 20\%$, and are listed in Table III. Upper limits on γ for the other possible primaries were estimated and are listed in Table III. The total width has been estimated² to be 0.3 kev, which is about one-quarter of the single-particle value,²⁰ and hence the values of γ discussed above are close to the partial widths for gamma emission.

418-kev Resonance

The measurement of the direct spectrum at this resonance was complicated by the presence of carbon contamination on the target, as well as by time-dependent background. The reaction $C^{12}(p, \gamma)N^{13}$ shows a resonance for a 2.37-Mev gamma ray at $E_p = 457$ kev, with a width of 40 kev.¹³ In order to subtract this gamma ray from the spectrum, measurements were made just below the resonance at 406 kev and at two energies on the maximum of the yield at 421 and 445 kev. The resulting 90° spectrum, also corrected for residual background with the beam off, is shown in Fig. 7(a). The following gamma rays are observed: 2.70 Mev, 2.25 Mev, 1.81 Mev, 1.36 Mev, and a complex of energy about 0.9 Mev. In addition, but not shown in Fig. 7(a), a complex of energy about 0.5 Mev was observed.

Coincidence spectra were measured in two different ways. First, with the counters set at 0° and 90°, respectively, and shielded from each other, one counter was gated to register gamma rays in coincidence with the

0.5-Mev complex, and gamma rays of energy 2.25 Mev, 1.36 Mev, and about 0.9 Mev were observed. Second, with the counters set at 90° and 270°, one counter was gated to register gamma rays in coincidence with the 0.9-Mev complex, and gamma rays of energy 1.81 Mev, 1.36 Mev, and about 0.9 Mev were observed. These two coincidence spectra are shown in Figs. 7(c) and 7(b), respectively.

From these measurements the decay scheme can be constructed as shown in Fig. 7(d). The 2.70-, 2.25-, and 0.89-Mev gamma rays are primaries feeding the ground state, the 0.45-Mev state, and the 1.81-Mev state, respectively. The measurements on the branching ratios of the 1.81-Mev state are consistent with the somewhat better determination described previously at the 1.49-Mev resonance. As can be seen from Fig. 7(d), there are actually three gamma rays of energy within 50 kev of 0.9 Mev, so that, again, this was not a suitable resonance for determining the branching ratio of the 0.95-Mev level.

Angular distribution measurements were made for both the ground state (2.70 Mev) transition and the transition to the 0.45-Mev state (2.25 Mev). This latter included the gamma ray of energy 2.37 Mev from the $C^{12}(p, \gamma)$ reaction, and the combined distribution is shown in Fig. 7(e). The angular distribution of the 2.70-Mev transition is shown in Fig. 7(f). The magnitude of the contribution of the carbon gamma ray was estimated as described above at 90°. Since it originates from a state of spin 1/2,¹³ its angular distribution will be spherically symmetric, and the result of this will be to change the P_2 coefficient from -0.3 to -0.5. Since the 0.45-Mev state ($J = \frac{1}{2}+$) is fed by a primary transition from the 2.70-Mev state, and the distribution is not spherically symmetric, the spin and parity of the capturing state must be 3/2± or 5/2+. As shown in Fig. 7(e), the 5/2+ assignment is eliminated by the distribution of the 2.25-Mev gamma ray even if no correction for the C^{12} contamination is made. The combination 3/2- for the capturing state is elimi-

²⁰ A. M. Lane, Atomic Energy Research Establishment, Harwell Report No. T/R 1289, 1954 (unpublished).

nated since the theory for $3/2^- \rightarrow 5/2+$ is $P_0 - \frac{1}{10}P_2$, assuming no $M2$ contribution to the $E1$. The measured value is $P_0 - (0.5 \pm 0.1)P_2$ for the 2.70-Mev ground-state transition, which requires the transition to be $3/2+ \rightarrow 5/2+$ with an $E2$ to $M1$ intensity ratio in the range 0.06 to 0.22 or 20 to 800, and zero phase difference. The measured distribution for the 2.25-Mev transition is $P_0 - (0.4 \pm 0.1)P_2$, and for $3/2+ \rightarrow 1/2+$ this corresponds to an $E2$ to $M1$ intensity ratio in the range 0 to 0.01 with zero phase difference or 3 to 7 with 180° phase difference.

The elastic scattering of protons by Mg^{24} showed no indication of the resonance at 418 kev.¹ No previous spin or parity assignments have been made for this level.

The branching ratios shown in brackets in Fig. 7(d) for the primary radiations were measured in a manner similar to that described for the previous resonance, using the above angular distributions for the 2.25- and 2.70-Mev gamma rays and a calculated distribution for the 0.89-Mev gamma ray, which assumed $M1$ radiation only. The upper limit on a possible primary transition to the 0.95-Mev state was estimated from the spectrum in coincidence with 0.5-Mev gamma rays [Fig. 7(c)].

The partial widths ($\gamma = \Gamma_p \Gamma_\gamma / \Gamma$) have been measured for the three primary radiations at this resonance, and are listed in Table III. The accuracies in this case are estimated to be $\pm 50\%$ because the H_s^+ beam was employed, and the relationship between the charge striking the target and the total number of protons depends on the extent to which the ion is stripped by residual gas in the system after being bent by the magnet. There is evidence at the 1.66-Mev resonance to be discussed later that the proton width of this 418-kev resonance is greater than the gamma-ray width, so the values of γ measured here are probably approximately equal to Γ_γ , the partial width for gamma emission.

825-kev Resonance

The direct spectrum measured at 90° at this resonance is shown in Fig. 8(a). Gamma rays of energy 3.09, 2.64, 2.14, 0.95, and 0.5 Mev were observed. The coincidence spectra shown in Figs. 8(b), 8(c), and 8(d) indicated that a gamma ray of about 0.5 Mev was in coincidence with that of 2.64 Mev, and gamma rays of energy 0.95 and about 0.5 Mev were in coincidence with that of 2.14 Mev. No gamma rays were observed to be in coincidence with the 3.09-Mev gamma ray. In these measurements the two counters were set at 90° and 270° , respectively, to the beam.

From these measurements the decay scheme of Fig. 8(e) can be constructed. The 3.09-, 2.64-, and 2.14-Mev gamma rays are primaries feeding the ground, 0.45-Mev, and 0.95-Mev states, respectively.

The spin and parity of this resonance are unambiguously determined from the elastic scattering data^{1,2} to be $3/2^-$. Theoretical P_2 coefficients for the angular distribution of $E1$ gamma-ray transitions from an

initial $3/2^-$ state to final states of spin and parity $1/2+$, $3/2+$, and $5/2+$ are -0.5 , $+0.4$, and -0.1 , respectively.¹⁶ The spectrum of the three primary radiations was measured at three angles, 0° , 45° , and 90° , and the areas under the total absorption peaks of the 3.09-, 2.64-, and 2.14-Mev gamma rays were determined, corrected in the case of the 2.14 for the tails of the 3.09 and 2.64, and in the case of the 2.64 for the tail of the 3.09. In making this correction the standard shapes of spectra were employed. The spectra at 0° and 90° are compared in Fig. 8(f). From these measurements, the experimental coefficient of P_2 for the 3.09-, 2.64-, and 2.14-Mev transitions was found to be -0.14 ± 0.04 , -0.48 ± 0.02 , and $+0.61 \pm 0.18$, respectively. Since the three lowest states of Al^{25} have even parity,³ this permits an unambiguous assignment of $5/2+$ and $3/2+$ for the ground state and second excited (0.95 Mev) state of Al^{25} , and confirms the assignment of $1/2+$ for the first excited state³ (0.45 Mev). It should be emphasized that these conclusions depend only on the assumption that $M2$ admixtures in the $E1$ transitions are negligible.

Shown in brackets in Fig. 8(e) are the branching ratios for the three primary transitions observed at this resonance, corrected as described previously. There was no evidence for a primary to the 1.81-Mev level. This would be an $E1$ transition of energy 1.28 Mev, and is

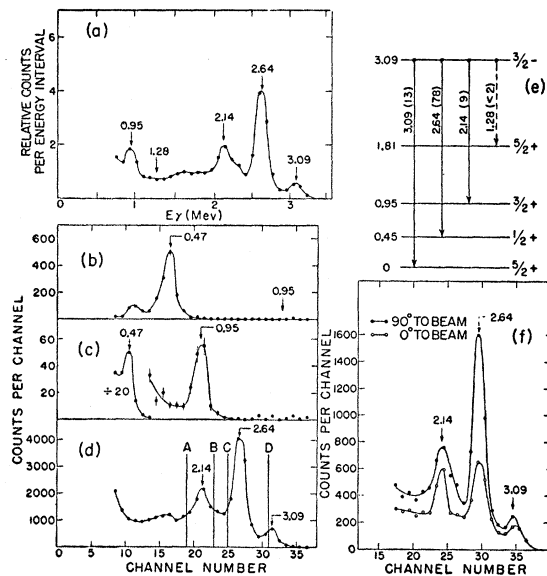


FIG. 8. Measurements at the 825-kev resonance. (a) A portion of the direct spectrum of gamma rays. The energies of the principal gamma rays are shown. (b) A portion of the spectrum of gamma rays in coincidence principally with gamma rays of 2.64 Mev. (c) A portion of the spectrum of gamma rays in coincidence principally with gamma rays of 2.14 Mev. (d) Part of the direct spectrum showing the limits A and B of the single-channel analyzer which gated the coincidence spectrum (c), and C and D which gated the coincidence spectrum (b). (e) The decay scheme for the 3.09-Mev state in Al^{25} . The gamma-ray energies are listed along with branching ratios in brackets. (f) The high-energy part of the direct spectrum of gamma rays measured at 0° and 90° to the proton beam.

estimated to be less than 15% of the ground-state transition.

The values of $\gamma = \Gamma_p \Gamma_\gamma / \Gamma$ measured at this resonance are listed in Table III, and have an estimated uncertainty of $\pm 20\%$. The total width has been estimated² to be 1.5 keV, which is about one-quarter of the single-particle value and therefore, as at the 1.49-MeV resonance, the measured values of γ are close to the partial widths for gamma emission.

1.20-MeV Resonance

This rather weak resonance in the reaction $Mg^{24}(p, \gamma)Al^{25}$, corresponding to a level at 3.44 MeV in Al^{25} , is found at a proton energy rather close to a resonance in the reaction $N^{15}(p, \alpha\gamma)C^{12}$ at $E_p = 1.210$ MeV with a width of 22.5 keV.¹³ This latter reaction gives rise to a gamma ray of energy 4.43 MeV, and sufficient nitrogen was present on the target to make a contribution comparable to that from the weak ground state transition of energy 3.44 MeV from the $Mg^{24}(p, \gamma)Al^{25}$ reaction. In addition, gamma rays of 6–7 MeV were present from fluorine contamination. The 90° direct gamma-ray spectrum shown in Fig. 9(a) was obtained by making measurements on and off the resonance in order to subtract the contamination radiations. It shows gamma rays of energy 3.44, 1.83, 1.61, and 0.51 MeV. Coincidence measurements shown in Figs. 9(b) and 9(c) established that the 1.83- and 1.61-MeV radiations were in cascade. The 0.51-MeV gamma ray is due to positron annihilation. The secondary peak observed in the coincidence spectrum [Fig. 9(b)], although somewhat higher than expected from single annihilation escape for a gamma ray of this energy, does not appear to indicate the presence of another gamma ray, and is probably the result of a statistical fluctuation.

The order of the cascading cannot be determined by these measurements. In the decay scheme of Fig. 9(d), it is assumed that the cascade proceeds via a state in Al^{25} at 1.61 MeV which has not previously been observed. Such a state would be analogous to the 1.61-MeV level in the mirror nucleus Mg^{25} .⁴

The angular distribution of the ground-state gamma ray (3.44 MeV) with respect to the proton beam was measured and is shown in Fig. 9(e). To obtain this distribution rather long runs (of the order of one hour for each angle) were required. The background subtraction discussed above accounts for the large standard deviations. The data show some evidence for the presence of a negative P_4 term²¹ and, this being so, the spin and parity of the 3.44-MeV level are either $9/2+$ or $5/2+$. Since the latter might be expected to show transitions to the 0.95- and 1.81-MeV states, the former is favored. If the capturing state is $9/2+$, a reasonable assignment for the 1.61-MeV state would be $7/2+$, explaining why it is preferred in the gamma-ray cascading.

²¹ Note added in proof.—Analysis by least squares of this distribution gives $a_2/a_0 = +0.33 \pm 0.06$ and $a_4/a_0 = -0.14 \pm 0.05$.

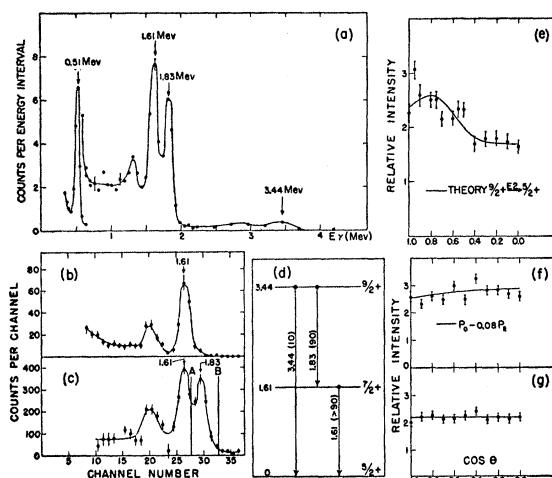


FIG. 9. Measurements at the 1.20-MeV resonance. (a) The direct spectrum of gamma rays. The energies of principal gamma rays are shown. (b) A portion of the spectrum of gamma rays in coincidence principally with gamma rays of 1.83 MeV. (c) Part of the direct spectrum showing the limits A and B of the single-channel analyzer which gated the coincidence spectrum (b). (d) The decay scheme for the 3.44-MeV state in Al^{25} . The gamma-ray energies are listed along with branching ratios in brackets. (e) The direct correlation of the 3.44-MeV gamma ray with respect to the proton beam. The solid line is the theoretical distribution $P_0 + (10/21)P_2 - (2/7)P_4$ which would arise from a $9/2+ \rightarrow 5/2+$ gamma transition. (f) The direct correlation of the 1.61-MeV gamma ray with respect to the proton beam with the intermediate 1.83-MeV radiation unobserved. (g) The direct correlation of the 1.83-MeV gamma ray with respect to the proton beam.

The angular distribution of the direct transition to the 1.61-MeV state, along with the distribution of the 1.83-MeV gamma ray with respect to the beam with the 1.61-MeV gamma ray unobserved, is shown in Figs. 9(f) and 9(g). Assuming the three states at 3.44 MeV, 1.61 MeV, and ground to be $9/2+$, $7/2+$, and $5/2+$, respectively, the $E2$ to $M1$ intensity ratio for the 1.83-MeV gamma ray lies in the range 0.01 to 0.03 with 0° phase difference, to give a distribution $P_0 + (0.0 \pm 0.1)P_2$; and that for the 1.61-MeV gamma ray is 0.02 to 0.06 with 180° phase difference, to result in the observed P_2 coefficient of -0.1 ± 0.1 . In both cases the other range of values for x^2 permitted by the observed coefficients of P_2 require large P_4 coefficients which are not observed experimentally.

The branching ratios for the two primary radiations are shown in brackets in Fig. 9(d), and the values of $\gamma = \Gamma_p \Gamma_\gamma / \Gamma$ in Table III. The probable errors for the listed values of γ are estimated to be $\pm 20\%$. Here, again, a spin of $9/2$ was assumed for the initial state.

The single-particle limit for a g -wave resonance at this energy would be about 4 eV. However, since other even parity resonances discussed below have widths considerably less than the single-particle value² by factors of the order of 500, one might expect the width of this resonance to be as small as 8×10^{-3} eV. Since this is the same order of magnitude as the measured values of γ , the gamma-ray partial widths cannot be obtained from these measurements.

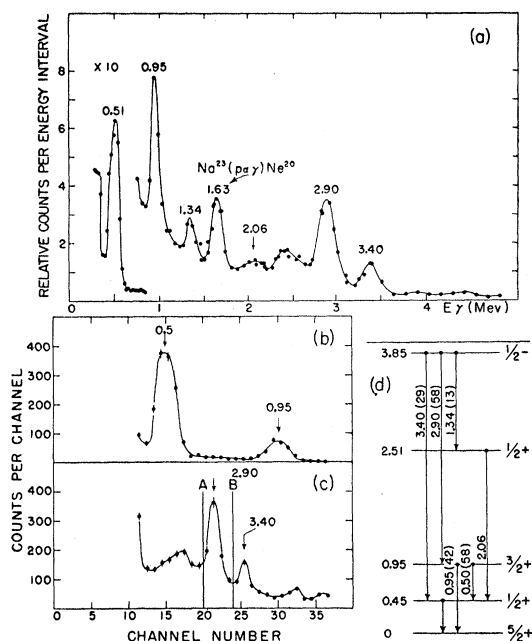


FIG. 10. Measurements at the 1.62-Mev resonance. (a) The direct gamma-ray spectrum. Energies of the principal gamma rays are shown. (b) Part of the spectrum of gamma rays in coincidence principally with gamma rays of 2.90 Mev. (c) Part of the direct spectrum showing the limits A and B of the single-channel analyzer which gated the coincidence spectrum (b). (d) The decay scheme for the 3.85-Mev state in Al^{25} . The gamma-ray energies are listed along with the branching ratios in brackets.

The level at 1.61 Mev was not observed by Goldberg,³ nor was the resonance at a proton energy of 1.20 Mev observed by Mooring *et al.*¹

1.62-Mev Resonance

The analysis² of the elastic scattering of protons¹ from Mg^{24} showed that this resonance has spin and parity $1/2^-$ and a total width of 36 keV. The direct 90° spectrum of proton capture gamma rays at the resonance is shown in Fig. 10(a). Since the resonance is so broad, the usual on-off resonance subtraction technique could not be applied, and some contaminant gamma rays are observed. The direct spectrum shows gamma rays of energy 3.40, 2.90, 1.34, 0.95, and 0.51 Mev. In addition, a gamma ray of energy 1.63 Mev is observed which is assumed to arise from the reaction $\text{Na}^{23}(p,\alpha\gamma)\text{Ne}^{20}$. There are also gamma rays of energy considerably higher than 3.4 Mev which may be from nitrogen and fluorine contamination. The coincidence spectrum of Figs. 10(b) and 10(c) shows that a 0.95-Mev and about a 0.5-Mev gamma ray are in coincidence with the 2.90-Mev. It was also shown that the 3.40-Mev gamma ray was in coincidence only with one of about 0.5 Mev. The 1.34-Mev gamma ray corresponds in energy to a primary transition to the level at 2.51 Mev in Al^{25} . This state is known⁸ to cascade primarily by a 2.06-Mev transition to the first excited state, and, as indicated on Fig. 10(a), the direct spectrum shows that

a gamma ray of this energy and of an intensity which is comparable to that of the 1.34-Mev appears. A coincidence spectrum with one counter gated on the 1.34-Mev gamma ray also showed the presence of a 2.06-Mev gamma ray. This suggests that the proton width of the 2.51-Mev level is equal to or less than the gamma widths.

The decay scheme based on these considerations is shown in Fig. 10(d). The gamma rays of energies 3.40, 2.90, and 1.34 Mev are primaries feeding the levels in Al^{25} at 0.45, 0.95, and 2.51 Mev, respectively.

A triple correlation was measured with one counter fixed at 270° to the beam and gated with its single-channel analyzer set on the 2.90-Mev gamma ray. The angular distribution of 0.95-Mev gamma rays in coincidence with those of 2.90 Mev was measured in the second counter between 0° and 90° . The result could be expressed as $P_0 + (0.0 \pm 0.1)P_2$.

From the coincidence spectrum measurements of Figs. 10(b) and 10(c) and the triple correlation obtained above, the branching ratio of the 0.95-Mev level in Al^{25} and the $E2-M1$ mixture of the 0.95-Mev radiation were obtained. The branching ratio of the 0.95-Mev state is 42% for 0.95-Mev radiation and 58% for 0.50-Mev. The intensity ratio for $E2-M1$ mixtures for the 0.95-Mev gamma ray is 0 to 0.06 with phase undetermined or 5 to 50 with zero phase difference. All the branching ratios measured at this resonance are shown in brackets on Fig. 10(d).

Absolute partial widths for the three primaries were measured and are listed in Table III. In this case the proton width of the level is much greater than the gamma widths and is about one-sixth of the single particle value, and hence the measured values of γ are close to Γ_γ . Again the estimated accuracy for values of γ is $\pm 20\%$.

1.66-Mev Resonance

As shown in the yield curve of Fig. 4, this resonance is narrow and is situated on the side of the broad 1.62-Mev resonance discussed in the foregoing. The direct spectrum shown in Fig. 11(a) was obtained by subtracting spectra observed just below the resonance from those measured at the maximum of the resonant yield. In this way gamma-ray transitions due to the broad resonance were eliminated.

The direct spectrum, which is quite complex, shows gamma rays of energy 3.88, 3.43, 2.93, 2.07, 1.81, 1.36, 1.18, 0.95, and 0.51 Mev, which can be ascribed to proton capture in Mg^{24} , and a gamma ray of 1.63-Mev energy which is probably due to sodium contamination.

Coincidence measurements were not made at this resonance because of the presence of the broad resonance, and hence the decay scheme shown in Fig. 11(b) is based on the direct spectrum of Fig. 11(a). The 3.88-, 3.43-, and 2.93-Mev radiations feed the ground, first, and second excited states respectively. The 2.07-Mev gamma ray has the correct energy to be a primary

transition to the 1.81-Mev state. It does not, however, have sufficient intensity to account for all the 1.81- and 1.36-Mev gamma rays observed in the direct spectrum, and it may be that a hitherto unobserved state is being fed. The 1.18-Mev transition could correspond energetically to a primary transition to the state at 2.70 Mev. If the proton width of this state were considerably greater than the gamma widths, no radiation subsequent to this transition would be observed. The fact that, for example, the 2.25-Mev gamma ray is not observed is consistent with this hypothesis.

The angular distributions of the three highest energy primary transitions were measured by recording the spectrum on and off the resonance at a series of angles between 0° and 90°. Figures 11(c) and 11(d) show the results for the 2.93- and 3.88-Mev gamma rays. The errors on the measurements for the 3.43-Mev gamma ray were quite high because of the large subtraction of the first escape peak from the ground state transition, and the results were useful only for obtaining the branching ratio.

Since the first three states of Al²⁵ are fed by primary transitions at this resonance, the spin and parity for the capturing state must be 1/2+, 3/2±, or 5/2+, assuming that only E1, M1, and E2 participate. The coefficient of P₂ observed in the direct correlation of the ground state transition has a value of 0.75±0.15, and this requires that the spin and parity of the 1.66-

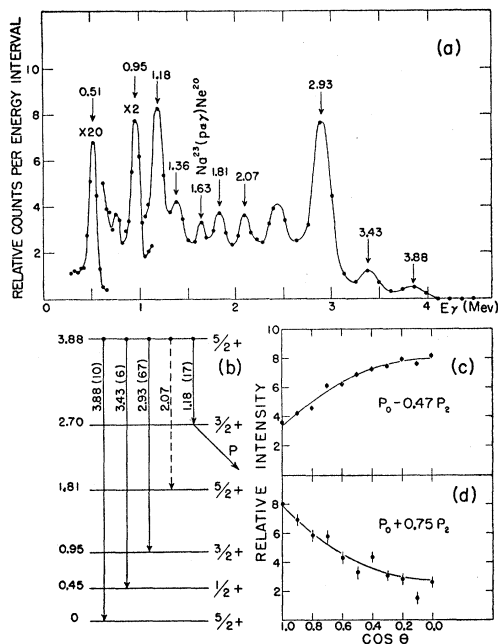


FIG. 11. Measurements at the 1.66-Mev resonance. (a) The direct gamma-ray spectrum. Energies of the principal gamma rays are shown. (b) The decay scheme for the 3.88-Mev state in Al²⁵. The gamma-ray energies are listed along with the branching ratios in brackets. (c) The direct correlation of the 2.93-Mev gamma ray with respect to the proton beam. (d) The direct correlation of the 3.88-Mev gamma ray with respect to the proton beam.

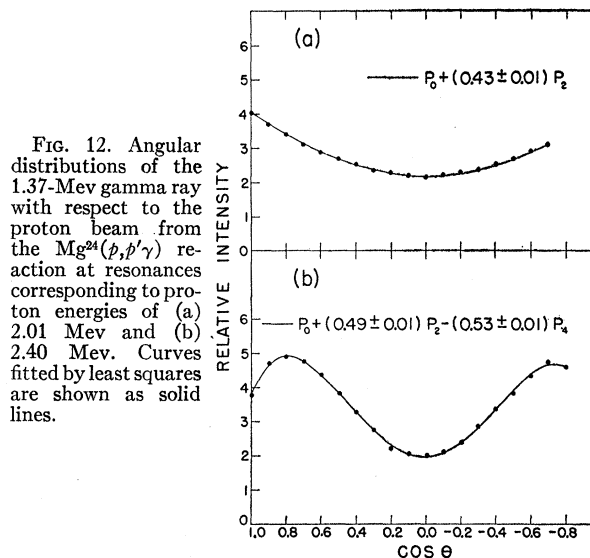


FIG. 12. Angular distributions of the 1.37-Mev gamma ray with respect to the proton beam from the Mg²⁴(p,p'γ) reaction at resonances corresponding to proton energies of (a) 2.01 Mev and (b) 2.40 Mev. Curves fitted by least squares are shown as solid lines.

Mev resonance be 5/2+. This is consistent with the analysis of the elastic scattering data,^{1,2} which required *d*-wave formation. The intensity ratio of the E2–M1 mixture for the 3.88-Mev gamma ray obtained from this angular distribution lies in the range 0.02 to 0.25, with 0° phase difference. The E2–M1 mixture for the 2.93-Mev transition determined from its distribution P₀–(0.47±0.05)P₂ [Fig. 11(c)] lies in the range 0 to 0.003 with 180° phase difference. The other range of values of *x*² permitted by the observed P₂ coefficient in the distribution of the 2.93-Mev gamma ray again requires a large coefficient of P₄, which is not observed. The 3.43-Mev gamma ray is an E2 transition.

The quantity $\gamma = \Gamma_p \Gamma_\gamma / \Gamma$ for the three highest energy primaries is listed in Table III, with estimated accuracies of ±20%. The total width² for this resonance is 100 ev, and since this is large compared to γ , the latter can be assumed to be close to Γ_γ in each case. Unlike the odd parity levels discussed previously, the total width of this resonance is only 0.2% of the single particle value.

2.01- and 2.40-Mev Resonances

Above 2 Mev, gamma rays from the reaction Mg²⁴(p,p'γ)Mg²⁴, Q=–1.37 Mev, dominate the spectrum, and it was the yield of these 1.37-Mev gamma rays that was measured for proton energies in the range from 2 to 3 Mev. Two very strong resonances are observed (Fig. 4) at proton energies of 2.01 and 2.40 Mev superimposed on a low but slowly rising background presumably produced by higher resonances.

The angular distributions of this 1.37-Mev gamma ray were measured at the peak of these two resonances, and are shown in Fig. 12. The analysis into a Legendre polynomial expansion up to P₄, including odd terms, showed that the only significant terms were the P₂ coefficient (0.43±0.01) at the 2.01-Mev resonance and

the P_2 (0.49 ± 0.01) and P_4 (-0.53 ± 0.01) coefficients at the 2.40-Mev resonance. When the P_2 coefficients are increased by 5% and the P_4 by 10% to correct for finite geometry, the distribution at the 2.01-Mev resonance is consistent only with a spin and parity for the resonance of $3/2 \pm$, and that at the 2.40-Mev resonance only with a spin and parity of $5/2 \pm$. The only assumption used in this analysis is that g -waves or higher are negligible for the inelastically scattered protons.

The analysis of the elastic scattering data^{1,2} showed that both resonances were formed by d -wave protons. Hence the assignments for the 2.01- and 2.40-Mev resonances are $3/2+$ and $5/2+$, respectively. In both cases, the inelastic protons are mostly s -wave, with perhaps up to 10% of d -wave admixture.

The values of $w\gamma = \Gamma_p \Gamma_{p'}/\Gamma$ for inelastic scattering, where $w = J + \frac{1}{2}$, are shown in Table III, and these correspond to values of γ of 30 and 117 ev, respectively, for the two resonances. It can easily be shown that the total width has a lower limit of 4γ , and hence must be greater than 120 and 468 ev, respectively, in the two cases. The analysis of the elastic scattering² data gave 150 and 300 ev for the two cases, but this was based on the assumption that inelastic scattering was negligible.

Proton capture gamma rays to low-lying states in Al²⁵ were observed at each of the two resonances, and values of $\gamma = \Gamma_p \Gamma_\gamma/\Gamma$ are given in Table III, again with estimated accuracies of $\pm 20\%$. Since the ratio of Γ_p/Γ is not known at either resonance, values of Γ_γ cannot be obtained, but are probably within a factor of two of the corresponding values for γ . Values for the P_2 coefficients in the angular distributions of the direct transitions to the 0.45- and 0.95-Mev levels were obtained at the 2.01-Mev resonance by measuring the spectrum at 0° and 90° . For the first transition, $3/2+ \rightarrow 1/2+$, $a_2/a_0 = -0.12 \pm 0.02$, and for the second, $3/2+ \rightarrow 3/2+$, $a_2/a_0 = +0.30 \pm 0.04$. From these values the $E2$ to $M1$ intensity ratio of the first transition is 0.033 ± 0.004 with zero phase difference, or 11 ± 1 with 180° phase difference, and for the second, 0.002 to 0.009 with 180° phase difference or 20 to 40 with zero phase difference.

At both resonances the total width is about 0.2% of

TABLE IV. Coefficients for the angular distributions of 1.37-Mev gamma rays from the reaction $\text{Mg}^{24}(p, p'\gamma)\text{Mg}^{24}$, $Q = -1.37$ Mev, expanded as a Legendre polynomial $W(\theta) = P_0 + (a_2/a_0)P_2 + (a_4/a_0)P_4$ at various proton energies. The standard deviation (S.D.) for each coefficient is also listed.

E_p Mev	a_2/a_0	S.D.	a_4/a_0	S.D.
2.10	0.261	0.02	0.174	0.02
2.47	0.373	0.02	0.157	0.02
2.71	0.367	0.01	0.197	0.01
2.72	0.428	0.01	-0.011	0.02
2.74	0.360	0.01	0.193	0.01
2.83	0.326	0.03	0.178	0.04
2.89	-0.033	0.03	-0.048	0.03
2.93	0.219	0.03	0.463	0.03
3.00	0.249	0.02	0.493	0.01

the single particle limit² for d -wave protons, which is the same value that obtained for the d -wave resonance at 1.66 Mev.

Resonances above 2.4 Mev

In addition to the 90° yield curve of 1.37-Mev gamma rays from the reaction $\text{Mg}^{24}(p, p'\gamma)\text{Mg}^{24}$, $Q = -1.37$ Mev, shown in Fig. 3, angular distributions of these gamma rays have been measured at several energies, both on the resonances at 2.72, 2.89, and 2.93 Mev, as well as between resonances at 2.10, 2.47, 2.71, 2.74, 2.83, and 3.00 Mev. Table IV lists the coefficients of P_2 and P_4 of the Legendre polynomial expansion of the data fitted by least squares on the Ferranti computer at the University of Toronto, for the various proton energies at which the distributions were measured. All but the last three were measured at 11 angles between 0° and 90° , while the last three were measured at 18 angles between 0° and 135° . Theory¹⁶ predicts that these distributions will have no odd Legendre polynomial terms, and none was observed in the last three distributions.

The distributions at 2.10, 2.47, 2.71, 2.74, and 2.83 Mev were measured on the slowly rising background underlying the narrower resonances at 2.01, 2.40, 2.72, 2.89, and 2.93 Mev. As shown in Table IV, all these distributions except at 2.10 Mev have similar coefficients of P_2 and P_4 . The fact that a P_4 term is observed indicates that a broad level of $J \geq 5/2$ is contributing to this background. A broad level at 3.14 Mev with a width of 200 kev was observed¹ in the yield of elastically scattered protons from Mg^{24} and assigned² spin and parity $3/2-$. When the P_2 and P_4 coefficients for the broad background are increased by 5% and 10%, respectively, to correct for geometry, they do not agree with the theoretical coefficients for direct distributions from $J = 5/2 \pm$, $7/2 \pm$, or $9/2 \pm$ (assuming outgoing g -wave protons negligible). Hence it is plausible to assume the presence of both a broad state of spin $3/2-$ and one with $J \geq 5/2$.

The angular distribution due to the resonance at 2.72 Mev can be obtained by the measurements made on the resonance and on each side at 2.71 and 2.74 Mev, if one can assume that the natural width of this resonance is smaller than the energy spread in the beam (~ 1 kev). If this is so, interference terms cancel, and a direct subtraction can be made since the relative intensities of the broad background and the narrow resonance can be obtained from the 90° yield curve. This yields $a_2/a_0 = 0.506 \pm 0.035$ and $a_4/a_0 = -0.255 \pm 0.038$ for the angular distribution of the narrow resonance at 2.72 Mev, and when the geometry correction is made this fits $5/2 \pm$, $7/2 \pm$, or $9/2 \pm$ within the errors. Hence it is possible to conclude only that the 2.72-Mev resonance has also a spin $\geq 5/2$.

When the angular distribution coefficients for the resonance at 2.93 Mev are corrected for geometry, the spin and parity for the capturing state are found to be

TABLE V. Comparison between experimental and theoretical $E1$ partial widths, based on the collective model, for gamma-ray transitions between the initial and final states shown in the first two columns.

Initial state Mev	Final state Mev	Theoretical Γ_γ ev	Observed Γ_γ ev
3.09 (3/2-)	0.45 (1/2+)	0.090	0.084
	0.95 (3/2+)	0.012	0.010
	1.81 (5/2+)	0.013	≤ 0.002
3.72 (7/2-)	1.81 (5/2+)	0.044	0.008
3.85 (1/2-)	0.45 (1/2+)	0.14	0.15
	0.95 (3/2+)	0.24	0.30

On this model, the ground state (5/2+), the 1.61-Mev state (7/2+), and the 3.44-Mev state (9/2+) constitute a rotational series with $K=5/2$. The positions of the states are fitted with a value of $3\hbar^2/I=1.626$ Mev, where I is the moment of inertia, and with vibration-rotation correction terms involving the squares of the spins ($\hbar\omega_\beta \sim \hbar\omega_\gamma \sim 11$ Mev).²⁵ Approximately the same values of the moment of inertia and of the vibration-rotation correction parameter also give the correct positions for the 0+, 2+, and 4+ states of Mg²⁴. The states at 0.45 (1/2+), 0.95 (3/2+), and 1.81 Mev (5/2+) would be a series with $K=\frac{1}{2}$ ($3\hbar^2/I=1.04$ Mev and $a=-0.025$), where a is the parameter defined by Bohr and Mottelson²⁶ for the positions of $K=\frac{1}{2}$ states. The states at 2.51 (1/2+), 2.70 (3/2+), and 3.88 Mev (5/2+) may possibly constitute a similar $K=\frac{1}{2}$ set ($3\hbar^2/I=0.914$ Mev and $a=-0.575$). Finally, the negative parity states at 3.09 (3/2-), 3.72 (7/2-), and 3.85 Mev (1/2-) may be a $K=\frac{1}{2}$ series resulting from the coupling of an $f_{7/2}$ particle to the core ($3\hbar^2/I=0.701$ Mev and $a=-3.16$). In all the cases of $K=\frac{1}{2}$ series, the value of vibration-rotation correction used was the same as for the series based on the ground state.

These hypotheses led to a search for the level at 3.44 Mev ($E_p=1.20$ Mev) which had not been observed in the proton scattering.¹ This fed the hitherto unobserved level at 1.61 Mev. Many of the branching ratios from the other resonances can also be explained in terms of this model. Ground-state $M1$ transitions from any of

²⁵ A. Bohr and B. R. Mottelson, in *Beta- and Gamma-Ray Spectroscopy*, edited by Kai Siegbahn (North-Holland Publishing Company, Amsterdam, 1955).

the $K=\frac{1}{2}$ series should be K -forbidden, and in fact seem to be attenuated by factors of approximately 20.

As an example, in Table V are compared the experimental and theoretical $E1$ partial widths for transitions between the negative parity series and the series based on the 0.45-Mev state, both having $K=\frac{1}{2}$. Two parameters were used to fit the results: $b=+0.07$, introduced by Alaga *et al.*,²⁶ which depends on the intrinsic wave function and is significant mainly in $K=\frac{1}{2} \rightarrow K=\frac{1}{2}$ transitions; and the electric dipole moment equal to 0.4×10^{-13} cm, which is about one-tenth of the moment for a single particle, $f_{7/2} \rightarrow d_{5/2}$ transition. The discrepancies may reflect admixtures of other values of K .

In the decay of the 3.44-Mev state (the 9/2+ member of the $K=5/2$ series based on the ground state), the $E2-M1$ intensity ratio has been measured for both the 9/2 \rightarrow 7/2 transition and the 7/2 \rightarrow 5/2 transition. They are, respectively, 0.01 to 0.03 and 0.02 to 0.06. The theoretical values are 0.03 and 0.02, using a quadrupole moment $1/\sqrt{5}$ times that derived from the level spacings, and a magnetic moment assuming that the coupled particle is in a $d_{5/2}$ state. The strong-coupling approximation has been assumed in these calculations.

The fact that many of the properties of low-lying levels in Al²⁵ can be described on the assumption of rotational bands suggests that marked collective effects may be playing a role in the neighborhood of mass number 25.

ACKNOWLEDGMENTS

We are indebted to Dr. L. G. Elliott, Dr. H. McManus, Dr. B. R. Mottelson, Dr. J. M. Kennedy, and Dr. D. A. Bromley for helpful discussions, to Mr. F. Goulding of the Electronics Branch for development of some of the circuits, to Mr. M. L. Smith and his associates of the E. M. Separator group at the Atomic Energy Research Establishment, Harwell, who supplied the Mg²⁴ deposited on special backings, to the Atomic Energy of Canada Limited Computing Section at the University of Toronto for fitting some of the curves with the FERUT computer, and finally to Mr. H. Smyth, Mr. P. J. Ashbaugh, and the operating staff for efficient running of the accelerator.

²⁶ Alaga, Alder, Bohr, and Mottelson, Kgl. Danske Videnskab. Selskab, Mat.-fys. Medd. 29, No. 9 (1955).